Effect of Pellet Size and Compatibilization on Thermal Decomposition Kinetic of Recycled Polyethylene Terephthalate/Recycled Polypropylene Blend

Supaphorn Thumsorn, Kazushi Yamada, Yew Wei Leong, Hiroyuki Hamada

Division of Advanced Fibro-Science, Kyoto Institute of Technology, Japan

Received 22 December 2010; accepted 28 June 2011
DOI 10.1002/app.35166
Published online 20 October 2011 in Wiley Online Library (wileyonlinelibrary.com).

ABSTRACT: This study considers the effects of pellet geometry and compatibilization on its moisture absorption and thermal degradation behavior of recycled polyethylene terephthalate (RPET) and recycled polypropylene (RPP) blend with the ultimate goal of optimizing the design of pellets to enhance their processability. The isoconversion of Flynn–Wall–Ozawa (FWO) was used for the kinetic study, which was suitable for thermal degradation of RPET/RPP blend in N_2 while the second order polynomial function was fitted for thermal oxidative degradation in air. Finer geometries, such as powders, were found to have higher moisture absorption rates due to their large surface area although they could also be easily dried. Furthermore, large surface area of fine powder as well as good interaction between RPP disperse particles and RPET matrix eased to decompose in the presence of oxygen thus accelerated chain breaking during thermal oxidative degradation especially at low heating rate. Meanwhile, larger pellets exhibited higher degradation activation energies, which suggest that they are more resistant to thermal degradation than smaller grains. © 2011 Wiley Periodicals, Inc. J Appl Polym Sci 124: 1605–1613, 2012

Key words: polymer blend; compatibilization; thermal decomposition kinetic; pellet size; moisture absorption

INTRODUCTION

Poly(ethylene terephthalate) (PET) is one of the most important commodity polymer materials due to its high performance, low cost, and excellent recyclability. Meanwhile, polypropylene (PP) is another commodity material that is commonly used to make caps for PET drinking bottles. The amount of waste that arise from postconsumer PET and PP especially in the beverage and packaging industry have stimulated in-depth investigation to produce innovative new products from recycled PET (RPET) and recycled PP (RPP) as a beneficial effort in reducing environmental pollution. Our previous work has proven the feasibility of recycling RPET and RPP simultaneously through melt extrusion while maintaining favorable mechanical properties through the usage of compatibilizers. It was also observed that the morphology of the extruded pellets would affect moisture absorption and subsequently the processability of the pellets. These pellets would then require drying prior to further processing, which would consume large amounts of energy and escalate production times. Therefore, it is important to reconsider the design of pellets, i.e., shape and size, to reduce drying time or, if possible, eliminate the drying process altogether.

Thermal degradation resistance of polymeric materials is also an important factor that affects productivity. Various kinetic models of thermal decomposition that consider isoconversion methods such as Flynn–Wall–Ozawa (FWO), Coast–Redfern, and Friedman[1–6] or peak degradation temperature such as Kissinger and Kim–Park[1,3,5,6] as well as free model fitting[7–10] can provide kinetic parameters such as activation energy (E_a), pre-exponential factor (A), and reaction order (n) to characterize the thermal stability and thermal decomposition mechanism of monotonic or filled polymeric materials.[1–6,11–16]

Thermal degradation stability and moisture absorption characteristics of thermoplastic materials are often thought to be related only to their chemical composition. However, the effect of disperse phase size in polymer blends on their thermal degradation characteristics is still not clearly understood. Furthermore, there is very little consideration about the effects of the various forms and sizes of thermoplastic raw materials, e.g., pellets, flakes, or powder, could have on their thermal degradation stability.

In this study, the effects of compatibilization and pellet size on the moisture absorption characteristics and thermal degradation kinetics of RPET/RPP blends were investigated. The isoconversion kinetic method of FWO or free model fitting was applied to elucidate the kinetic parameters by using

Correspondence to: S. Thumsorn (nooh17@yahoo.com).

thermogravimetric analysis data. The ultimate goals for this study are to suggest the most suitable pellet size and compatibilizer content to minimize moisture absorption and thermal degradation during processing of RPET/RPP blends.

EXPERIMENTAL

Materials

RPET and RPP in the form of flake (from crushed waste bottles) were provided by Yasuda Sangyo Co., Ltd, Japan. A styrene-ethylene-butadiene-styrene base compound was used as compatibilizer which purchased from JSR Corp., Japan. The ratio of RPET/RPP blend was set at 95/5. The amount of the compatibilizer was fixed at 5 phr. The blend without compatibilizer also prepared for the comparison.

Sample preparation

The blends were prepared by single screw extruder (SRV-P70/62, Nihon Yuki Co., Ltd., Japan). RPET was dried by using a dehumidifying drier at 120°C for 5 h before being fed into the extruder set at a barrel temperature of between 260 and 285°C and screw speed of 50 rpm. The extrudate was then pelletized into cylindrical-shaped pellets that are typically around 2 mm in diameter and 3 mm in length.

Grinding and sizing of pellets

The pellets were ground by using a power mill (PM-2005, Osaka Chemical Co., ltd., Japan) with a blade rotation speed of 38,000 rpm. The ground pellets were then sieved through stainless steel mesh with mesh sizes of 20, 40, and 60 that correspond to openings of 0.853, 0.422, and 0.251 mm, respectively. Liquid N_2 was used to cool the grinder and pellets during grinding to obtain smaller particles as well as to prevent morphological changes to the pellets. These pellets will then be referred to as 20 Mesh, 40 Mesh, and 60 Mesh, respectively, whereas un-ground pellets are known as "as-received" pellets.

Moisture absorption characterization

The pellets were dried in a convection oven set at 80°C for at least 8 h. The initial moisture content in the pellets was measured by using a KEM MCU610 Karl-Fischer moisture measurement system. The pellets were then subjected to moisture absorption in a EcoDryer™ humidity chamber provided by Itswa Co., Ltd., Japan. The temperature and relative humidity (RH) was set at 70°C and 80%, respectively. The pellets were removed from the chamber at 30 min intervals and the moisture content measurements were obtained immediately.

Morphology observation

Morphological analysis of ground powder and as-received pellet were performed by using a scanning electron microscope (JEOL/JSM-5200) set at 20 kV. Gold was sputtered onto the specimens for electron conductivity. The image J program was used to measure the sizes of the ground powders

Thermal degradation kinetics

The pellets were subjected to thermogravimetry analysis (TGA) by using a TA Instruments TGA2950 analyzer. The heating rate was varied at 2, 5, 10, and 20 °C/min in nitrogen and air. The various thermograms were used to determine the temperature at certain weight losses from 2.5 to 50% in accordance to the isoconversion of FWO method[1–6] that is based on the Arrhenius equation on the first order kinetic by

$$k(T) = A \exp\left(\frac{-E_a}{RT}\right) \tag{1}$$

where $k(T)$ is rate of reaction, E_a is activation energy (J/mol), A is the pre-exponential factor, T is temperature (K), and R is a universal gas constant (8.314 J/mol K).

The conversion of sample (α) at linear heating rate is defined as

$$\alpha = \frac{m_0 - m_T}{m_0 - m_{\text{final}}} \tag{2}$$

where m_0 is initial mass, m_T is mass at decomposition temperature, and m_{final} is mass at final decomposition reaction.

The solid-state decomposition for kinetic study[7–9] can be described by

$$\frac{d\alpha}{dt} = k(T) f(\alpha) \tag{3}$$

Therefore, the thermal decomposition kinetic based on the Arrhenius equation and the solid-state decomposition is written as follows:

$$\frac{d\alpha}{dt} = A \exp\left(\frac{-E_a}{RT}\right) f(\alpha) \tag{4}$$

For the kinetic study of nonisothermal experiments, eq. (3) is rewritten by

$$\frac{d\alpha}{dT} = \frac{A}{\beta} \exp\left(\frac{-E_a}{RT}\right) f(\alpha) \tag{5}$$

where β is the heating rate and $\beta = \frac{dT}{dt}$.

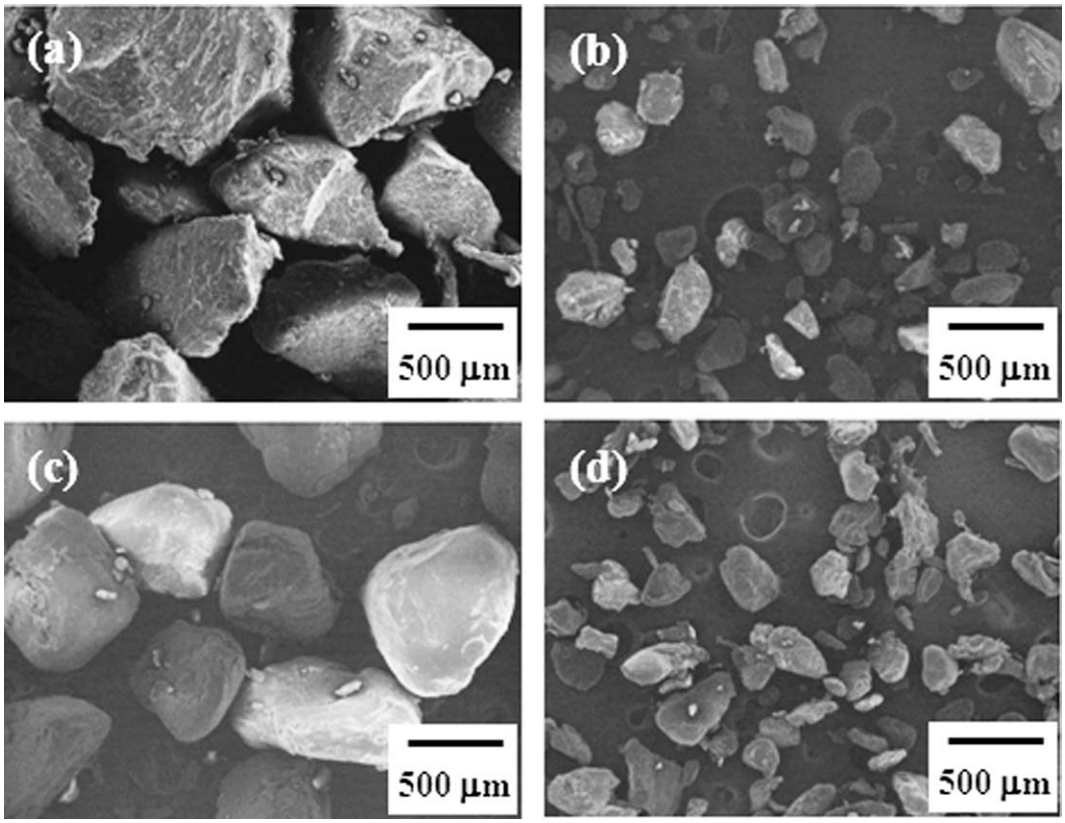

Figure 1 SEM photographs of ground pellet of (upper) uncompatibilized RPET/RPP blend (a) 20 Mesh, (b) 60 Mesh and (lower) compaitibized blend, (c) 20 Mesh, and (d) 60 Mesh.

The isoconversion kinetic method is widely used for thermal decomposition kinetic study. The basic assumption of this method is related to the reaction model, which is independent on temperature and heating rate.[7] The isoconversion of FWO method was selected. The FWO method involves measuring the degradation temperatures corresponding to values of weight loss during decomposition (α), which the FWO kinetic method can be assigned by using the Doyle approximation[2,3] in the form of

$$\log \beta = \log \frac{AE_a}{f(\alpha)R} - 2.315 - \frac{0.457\,E_a}{RT} \qquad (6)$$

Therefore, the slope of the plot between log heating rate and inverse temperature was used to determine the activation energy (E_a) for FWO thermal decomposition kinetic by

$$E_a = \frac{-R}{0.457}\left[\frac{d\log\beta}{d(1/T)}\right] \qquad (7)$$

RESULTS AND DISCUSSION

Figure 1 presents SEM photographs of uncompatibilized and compatibilized RPET/RPP blends after grinding of 20 Mesh and 60 Mesh ground powders. It can be seen that the ground pellets were irregular in shape and exhibited rough surfaces, especially in uncompatibilized blends. Figure 2 presents the morphology of the blends as observed from the surfaces of 20 Mesh and 60 Mesh pellets with and without compatibilizer. The SEM photographs revealed that the spherical RPP dispersed particles in uncompatibilized blends were much larger than those found in compatibilized blends, which the average size of RPP disperse particles are tabulated in Table I. Therefore, it was considered that the presence of compatibilizers provided finer and better dispersion of RPP in the RPET matrix. It is interesting to note that there is less of an exposure of RPP on the surface of as-received pellets while extensive exposure was found in ground pellets. Moreover, the grinding of the RPET/RPP pellets affected on surface morphology and surface roughness of the blend, especially the exposed of RPP particle on the surface.

Effect of pellet size on moisture absorption characteristics

Figure 3 shows the moisture absorption characteristics of the as-received pellets as compared to pellets ground to various mesh sizes for uncompatibilized and compatibilized blends. From the results, the size

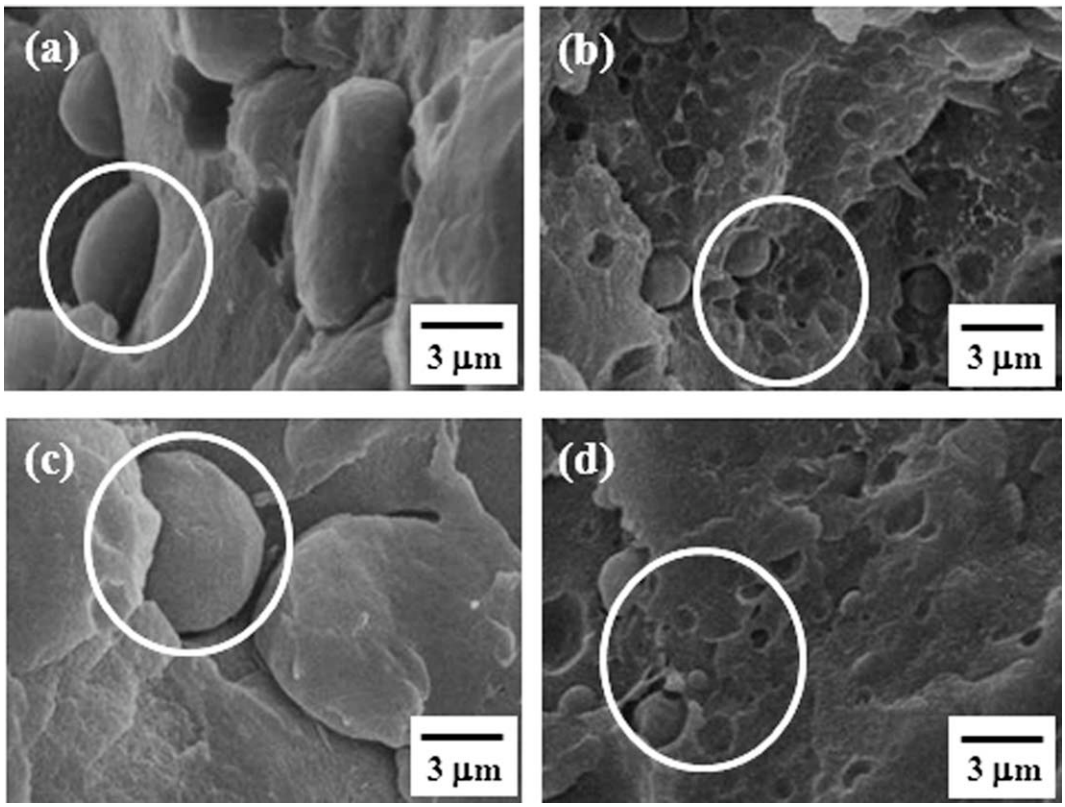

Figure 2 Morphology of ground pellet of (upper) uncompatibilized RPET/RPP blend (a) 20 Mesh, (b) 60 Mesh and (lower) compaitibized blend, (c) 20 Mesh, (d) 60 Mesh. RPP dispersed particles are indicated by circle.

of pellets has a more profound influence on the extent of moisture absorption as compared to compatibilization. The initial moisture content of the as-received pellets was slightly higher than the ground powders, which indicates the difficulty of drying the large pellets. When exposed to moisture, however, substantial moisture uptake in the ground pellets could be observed while the as-received pellets recorded a more gradual increment in moisture content. The significantly higher moisture uptake rate of the ground pellets could be attributed to their larger surface area. Moreover, it is possible that the rough surfaces due to grinding could have created higher surface energies, which attracted more water molecules, as compared to the smooth surface of the as-received pellets.

Effect of pellet size on thermal stability and decomposition kinetics

Figure 4 shows the material conversion curves during decomposition of the 20 Mesh uncompatibilized pellets exposed to different heating rates in nitrogen and air atmospheres. Single-step degradation curves could be observed when the materials were degraded in nitrogen as shown in Figure 4(a), while two-stage conversion curves were evident when the materials were exposed to air as shown in Figure 4(b). The first stage of conversion between 200 and 450°C was related to the major degradation stage of PET, which is attributed to chain scission of ester-linkage leading to decomposition of PET backbone and formation of char whereas the second stage of conversion between 450 and 600°C was caused by the decomposition of residual char.[17] The conversion curves would shift towards higher temperatures with increasing heating rate, which is due to the lag in heat transfer within the sample during decomposition. In addition, it was corresponding to the response of sample during decomposition at different heating rate whereby at high heating rate, materials could not decompose thoroughly and exhibited high degradation temperature and high rate of degradation.[18] However, the rates of conversion ($d\alpha/dt$) in the blends, as presented in Figure 5, do not vary significantly when comparing samples

TABLE I
The Average Size of RPP Dispersed Particle in RPET/RPP Blends Without and with Compatibilizer

Size	Uncompatibilized blend	Compatibilized blend
As-received	4.99 ± 0.69	0.77 ± 0.14
20 Mesh	4.95 ± 0.98	0.71 ± 0.23
40 Mesh	4.93 ± 0.84	0.67 ± 0.18
60 Mesh	4.71 ± 0.78	0.73 ± 0.16

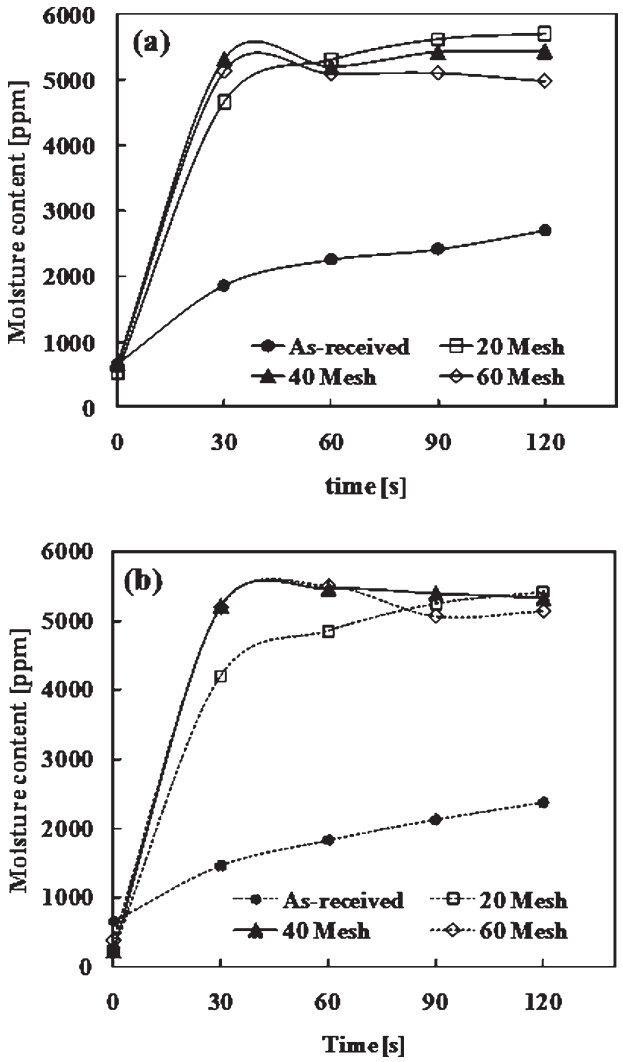

Figure 3 Moisture absorption characteristic of (a) uncompatibilized and (b) compatibilized RPET/RPP blend.

that were degraded in N_2 and air at a particular heating rate.

The pellet size and compatibilization did not have any significant effect on both the onset degradation temperature ($T_{d\ \text{onset}}$) at 5% sample weight loss and peak degradation temperature ($T_{d\ \text{peak}}$) of RPET/RPP blend when they were exposed to N_2 atmosphere, as can be seen in Table II. However, the $T_{d\ \text{onset}}$ and $T_{d\ \text{peak}}$ values were significantly lower when the specimens were exposed to air as opposed to N_2 irrespective of the presence of compatibilizers. Furthermore, the $T_{d\ \text{onset}}$ and $T_{d\ \text{peak}}$ values would further deteriorate with the reduction in pellet size from as-received to 60 Mesh. It is considered that smaller size pellets would acquire larger surface areas, leading to faster heat transfer and more drastic degradation than it would be in larger pellets. Also, the accelerated degradation in air is attributed to the thermo-oxidative degradation of the RPP phase, which can be apparently delayed through the incorporation of compatibilizers. With compatibilization, the RPP particles were more finely dispersed in the RPET matrix, which reduces the total area of exposure to oxidative degradation. This phenomenon can be discussed by using the thermal decomposition kinetic model in greater detail.

Thermal decomposition kinetic in nitrogen

Thermal decomposition kinetic is a useful tool for clarifying the mechanism of thermal degradation and thermal resistance of polymeric materials.[1,4,5] E_a values obtained from the kinetic study represent the potential parameter of thermal degradation/decomposition reaction, which can be used to gauge the susceptibility of the RPET/RPP blend to degradation during drying, melt processing, disposal, or recycling. The variation in E_a values during thermal decomposition reaction can be affected by pellet size, compatibilization as well as disperse phase

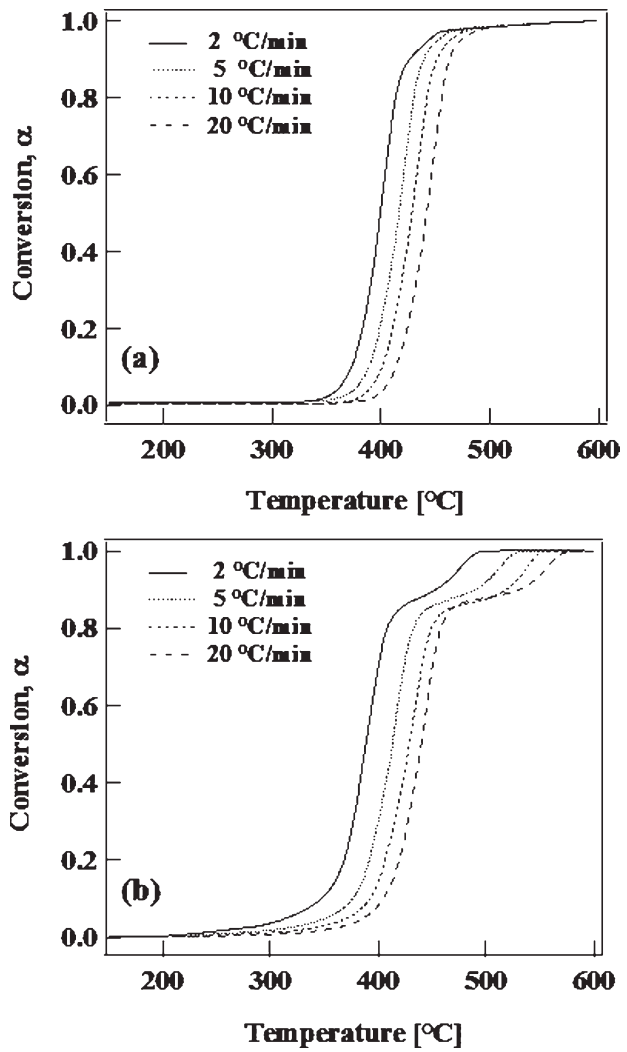

Figure 4 Weight loss conversion of 20 Mesh ground powder of compatibilized blend in (a) N_2 and (b) air.

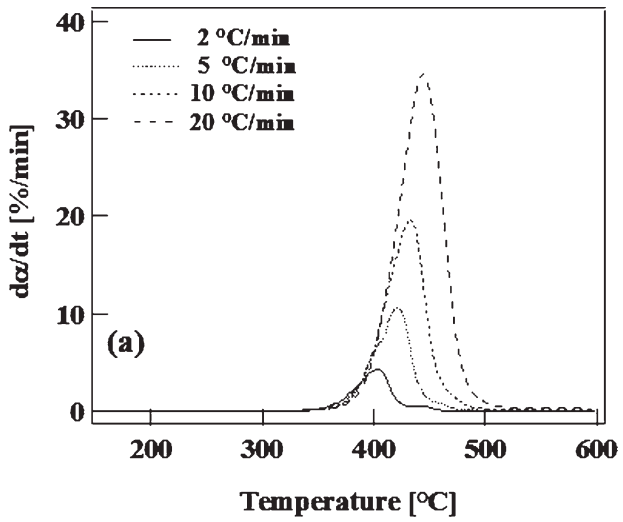

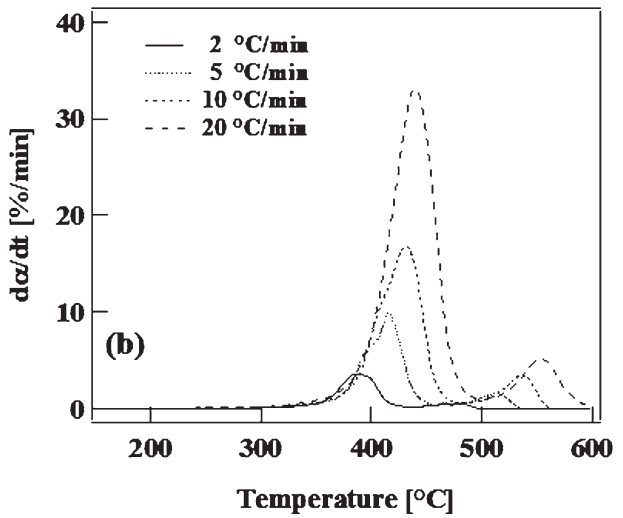

Figure 5 Rate of degradation ($d\alpha/dt$) of 20 Mesh ground powder of compatibilized blend in (a) N_2 and (b) air.

size. Therefore, small pellet would be ease to decompose due to its large surface area. Good adhesion and dispersion of RPP dispersed phase on RPET matrix could aid to resist thermal decomposition. Therefore, nonisothermal kinetic models such as the FWO method have been used for investigating the kinetic parameter of thermal decomposition of

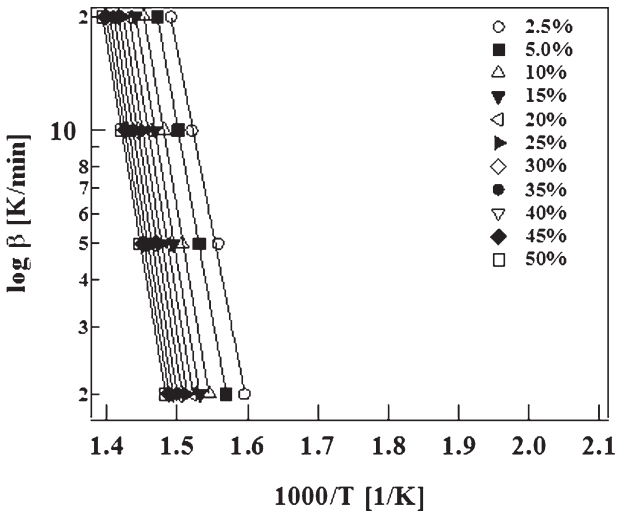

Figure 6 Flynn–Wall–Ozawa plot of 20 Mesh of compatibilized blend decomposition in N_2.

RPET/RPP blends. Figure 6 shows an example of the FWO plots for a 20 Mesh sample degraded in N_2 atmosphere. It is apparent that the FWO plots between the log β and $1/T$ are linear. The slopes of these plots can then be used for calculating E_a.

Figure 7 shows the effect of compatibilizer and pellet size on E_a values of RPET/RPP blends when degraded under N_2 atmosphere and the results are summarized in Table III. E_a values of as-received pellet for compatibilized blends were found to be higher than the blends without compatibilizer. It was mentioned earlier that the incorporation of compatibilizers could delay thermal degradation by increasing both the $T_{d\ \text{onset}}$ and $T_{d\ \text{peak}}$ values. Moreover, the fine dispersion and small size of RPP resisted thermal decomposition of RPET. In addition, the results tabulated in Table III show an increment in E_a values with decreasing pellet size. The large surface area of smaller pellet size was beneficial to sustain and prevent the volatile substance during decomposition thus resulting in enhanced thermal stability and present high E_a values. In Figure 7, the E_a values of various blends were similar irrespective of the degree of decomposition. The E_a values increased gradually at the initial stage of decomposition until

TABLE II
Onset and Peak Degradation Temperature of RPET/RPP Blends Without and with Compatibilizer in N_2 and Air at Heating Rate of 10 °C/min

	Uncompatibilized blend				Compatibilized blend			
	N_2		Air		N_2		Air	
Size	$T_{d\ \text{onset}}$ (°C)	$T_{d\ \text{peak}}$ (°C)	$T_{d\ \text{onset}}$ (°C)	$T_{d\ \text{peak}}$ (°C)	$T_{d\ \text{onset}}$ (°C)	$T_{d\ \text{peak}}$ (°C)	$T_{d\ \text{onset}}$ (°C)	$T_{d\ \text{peak}}$ (°C)
As-received	395.1	432.7	379.9	429.8	394.7	432.8	388.6	435.2
20 Mesh	395.7	436.5	363.2	429.9	393.4	433.5	371.6	430.6
40 Mesh	394.9	436.2	359.7	428.6	392.1	432.2	365.4	429.0
60 Mesh	394.3	434.9	341.4	430.1	392.6	432.3	338.9	424.8

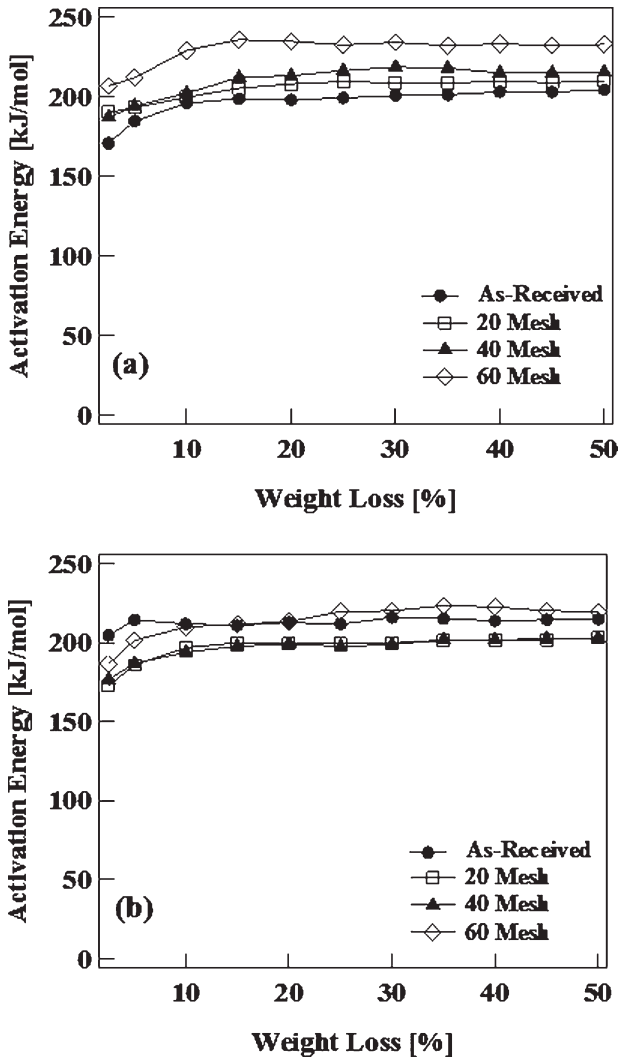

Figure 7 Activation energy of the blends (a) uncompatibilized and (b) compatibilized blend in N_2.

10% weight loss ($\alpha = 0.1$) thereafter the weight loss remained almost constant. The initial stage of thermal degradation in the presence of N_2 is attributed to depolymerization due to random chain scission and hydrolysis of ester-linkage. The primary degradation products of RPET would then cause a secondary degradation process including decarboxylation, hydrogen transfer, or transesterification.[14] The constant E_a value at the second step of decomposition indicates that thermal degradation of the blend presented similar mechanism and represented as apparent E_a value of the blends.

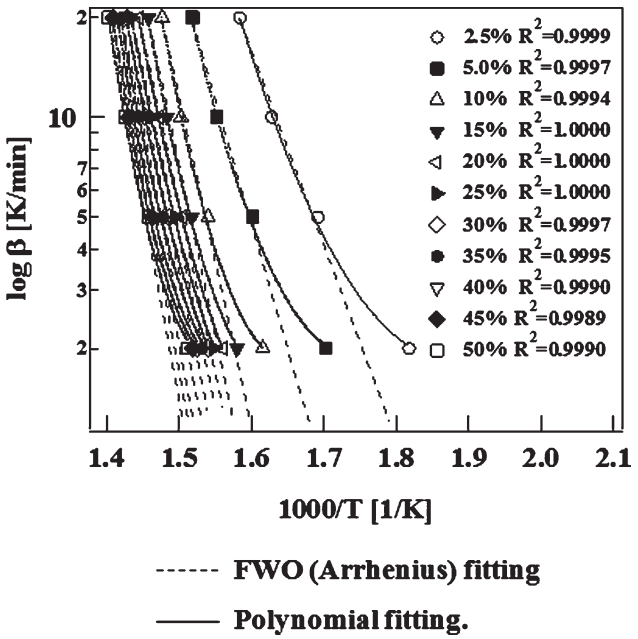

Figure 8 Flynn–Wall–Ozawa plot of 20 Mesh of compatibilized blend decomposition in air.

Thermal decomposition kinetic in air

Unlike in N_2, the effect of compatibilization and pellet sizes of RPET/RPP on thermal decomposition kinetic could be observed when the samples were exposed to air. The thermal oxidative degradation of the blend would conform to the nonlinear relationship, as can be seen from the FWO plots shown in Figure 8. From the results, a fitting model of the experimental data was done to establish the relationship of nonlinear regression of log β and $1/T$ and obtain the E_a values of thermal oxidative degradation. Figure 8 shows the FWO plots and fitting results of the compatibilized blend at with pellet size of 20 Mesh. It can be noted that the FWO plots of thermal oxidative degradation were influenced by heating rate, pellet surface area, and the size of RPP disperse phase in the blends. The FWO plots for the

TABLE III
Activation Energy of RPET/RPP Blends Without and with Compatibilizer in N_2 and Air

	Uncompatibilized blend				Compatibilized blend			
	$E_{a0.05}$ (kJ/mol)		$E_{a0.50}$ (kJ/mol)		$E_{a0.05}$ (kJ/mol)		$E_{a0.50}$ (kJ/mol)	
Size	N_2	Air	N_2	Air	N_2	Air	N_2	Air
As-received	184.6	196.5	204.3	201.3	214.4	157.5	214.9	192.9
20 Mesh	193.0	129.1	209.6	185.5	185.8	136.8	203.0	216.4
40 Mesh	193.8	119.8	215.4	185.5	186.8	82.3	202.9	178.0
60 Mesh	212.0	157.5	232.7	200.3	201.4	70.3	219.6	184.9

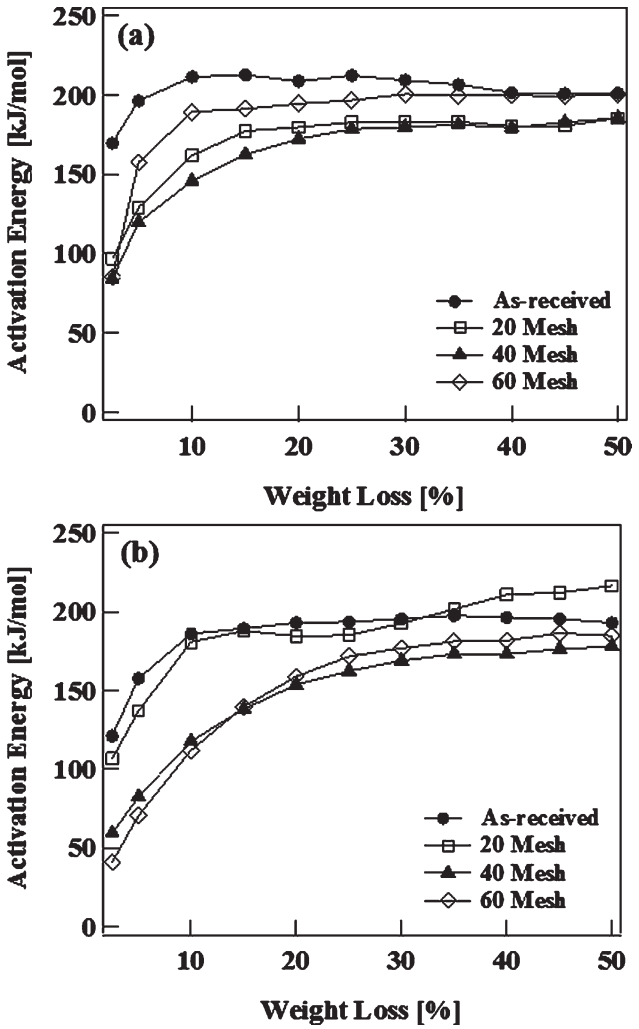

Figure 9 Activation energy of the blends (a) uncompatibilized and (b) compatibilized blend in air.

20 Mesh pellets would fit well to the following second order polynomial function (quadratic equation), irrespective of blend composition. The fitting equation can be described as:

$$\log \beta = a\left[\frac{1}{T}\right]^2 + b\left[\frac{1}{T}\right] + c \qquad (8)$$

where a is polynomial coefficient, b is linear coefficient, and c is constant. The E_a values can be obtained from the coefficient of nonlinear fitting plots, which are presented in Figure 9.

Figure 9(a,b) show the E_a values as a function of weight loss during thermal degradation in air for uncompatibilized and compatibilized blends, respectively. Based on the summary of E_a values in Table III, the thermal stability of uncompatibilized blends were slightly higher than that of compatibilized blends. It is thought that the larger RPP disperse particles in uncompatibilized blends were more able to resist thermal oxidative degradation, which could be due to small surface area of large RPP dispersed particles. Nevertheless, smaller pellets would degrade easier and faster due their larger surface area, especially at low heating rates. It is important to note that the RPET/RPP blends would be more thermally stable when the RPP disperse phase is not exposed to air since it is more prone to oxidative degradation. Therefore, it is preferable that the RPP, being the minor phase, be embedded in the RPET matrix so that the matrix can act as a protective barrier to prevent oxidation of RPP. The grinding of pellets into smaller sizes, however, could have exposed the RPP phase, which significantly expedites the thermal decomposition kinetic and thermal stability of the pellets. This explains the lower E_a values generated by the smaller pellets.

CONCLUSIONS

The effects of pellet size and compatibilization on moisture absorption and thermal degradation characteristics of RPET/RPP blends were elucidated. It was found that smaller pellets could easily absorb moisture due to their large surface area and their surface roughness. Therefore, smaller pellets were more susceptible to hydrolysis when exposed to high temperatures, especially in the presence of O_2. Conversely, these fine pellets would also dry quickly and more thoroughly than larger pellets under similar drying conditions. The FWO method was able to provide the activation energy for decomposition of the blends in the presence of N_2 while the model fitting method by using the second order polynomial function was more suitable to evaluate the thermal oxidative degradation of the blends in air. The size of the pellets and the compatibilization of the blends would significantly affect thermal decomposition kinetics. Large RPP dispersed phase particles in uncompatibilized blends were able to provide better thermal stability than finer particles in compatibilized blends due to its small surface area for oxidative decomposition of the blend. Moreover, it is considered that large pellet sizes were more resistant to thermal degradation as compared to smaller pellets. This could be attributed to the grinding of larger pellets into smaller grains, which could have exposed the RPP dispersed phase to oxidative degradation.

The authors gratefully acknowledge Dr. Hiroyuki Inoya, Yasuda Sanyo Co., Ltd., Japan for supporting materials and compounding system and Dr. Minoru Ogasahara, Itswa Co., Ltd., Japan for Karl-Fischer moisture measurement system.

References

1. Tang, W.; Liand, X.; Yan, D. J Appl Polym Sci 2004, 91, 445.
2. Dias, D.; Crespi, M.; Ribeiro, C.; Fernandesand, J.; Cerqueira, H. J Therm Anal Calorim 2008, 91, 409.

3. Kim, J.; Kimand, D.; Kim, S. Polym Compos 2009, 30, 1779.
4. Girija, B.; Sailajaand, R.; Madras, G. Polym Degrad Stab 2005, 90, 147.
5. Paikand, P.; Kar, K. Polym Degrad Stab 2008, 93, 24.
6. Kimand, S.; Park, J. Thermochim Acta 1995, 264, 137.
7. Vyazovkinand, S.; Wight, C. J Phys Chem A 1997, 101, 8279.
8. Khawamand, A.; Flanagan, D. J Phys Chem B 2006, 110, 17315.
9. Budrugeac, P. J Therm Anal Calorim 2009, 97, 443.
10. Chrissafis, K. J Therm Anal Calorim 2009, 95, 273.
11. Sahaand, B.; Ghoshal, A. Chem Eng J 2005, 111, 39.
12. Turmanova, S.; Genieva, S.; Dimitrovaand, A.; Vlaev, L. Express Polym Lett 2008, 2, 133.
13. Encinarand, J.; Gonz lez, J. Fuel Process Technol 2008, 89, 678.
14. Acar, I.; Pozanand, G. S.; Özgümüş, S. J Appl Polym Sci 2008, 109, 2747.
15. Sarrabi, S.; Colinand, X.; Tcharkhtchi, A. J Appl Polym Sci 2010, 118, 980.
16. Sánchez-Jiménez, P. E.; Pérez-Maqueda, L. A.; Perejón, A.; Criado, J. M. J Phys Chem A 2010, 114, 7686.
17. Dziçio[swsl]land, M.; Trzeszczyński, J. J Appl Polym Sci 1998, 69, 2377.
18. Wongsiriamnuayand, T.; Tippayawong, N. Bioresour Technol 2010, 101, 5638.